# Fast Dynamic Field-Oriented Control Using Direct Large Voltage Vector and Hysteresis Switch

Hasan Ali Gamal Al-kaf[1], and Kyo-Beum Lee[1]
[1] Department of Electrical and Computer Engineering, Ajou University, Suwon, South Korea

***Abstract*-- Field-oriented control (FOC) has been widely used for controlling the current control of permanent magnet synchronous motors (PMSMs) due to its excellent performance in steady-state operation. FOC suffers from slow dynamic response, as a result, its practical use may be limited for applications that require a very fast dynamic response. Accordingly, in this paper, a fast dynamic FOC (FFOC) for PMSM based on a real voltage vector and hysteresis switch is proposed. The hysteresis switch uses FOC in steady-state and the direct real voltage vector in transient-state. Simulation results show that the proposed model has similar steady-state performance as FOC. In addition, FFOC shows faster dynamic performance when FOC and model predictive control (FOC-MPC) are combined using hysteresis switch.**

***Index Terms*— field-oriented control, hybrid model, model predictive control, PMSM.**

## I. Introduction

The trend towards more energy-efficient and high-performance electric drive systems has resulted in the widespread adoption of permanent magnet synchronous motors (PMSMs) in various industrial applications. PMSMs have many advantages over traditional induction motors, including higher torque, better power density, compact size, and weight, low cost, and high efficiency, making them ideal for use in demanding applications that require excellent dynamic response. In addition, PMSMs offer a high degree of precision, making them a preferred choice for applications that require precise speed and position control such as automotive, aerospace, robotics, and renewable energy. The stator current directly affects the dynamic and steady-state performance of PMSM drives [1]. Therefore, a high-performance current controller is highly desirable.

The most popular current control schemes for PMSM drives are field-oriented control (FOC) and direct torque control (DTC). FOC is known for having a good steady-state performance which has zero average steady-state error, which can result in highly accurate control. However, FOC requires involved tuning of the parameters and various frame transformations. Moreover, the bandwidth is also limited, which may not be suitable for some high-performance applications that require very fast dynamic responses. On the other hand, DTC considers a fast dynamic method, which can be useful in applications where high-speed performance is essential. However, there are some drawbacks to DTC, including variable switching frequency, Moreover, high torque ripples may be present in DTC, which can reduce overall performance and efficiency [2]–[4].

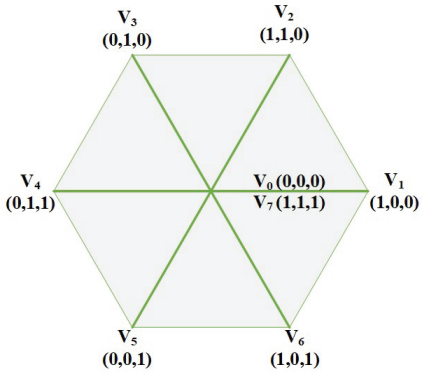

Fig. 1. Two-level space vector diagram.

In recent years, model predictive control (MPC) has emerged as a promising option for industrial motor drive applications, thanks to its simple concept, easy implementation, multivariable control, and its fast dynamics[5]–[7]. Despite its many advantages, classical MPC has some limitations that can reduce its overall performance. For example, it has a high dependence on system parameters, which can make it more challenging to implement and tune effectively, particularly in situations where parameter variations are present. Additionally, the variable switching frequency and limited number of voltage vectors (VVs) associated with classical MPC can lead to poorer steady-state performance when compared to FOC.

To address the limitations of classical MPC in PMSM control, researchers have developed advanced MPC algorithms that combine with other control strategies, such as discrete space vector modulation (DSVM), to improve performance and efficiency. The resulting MPC-DSVM algorithm can synthesize a wide range of virtual voltage vectors, leading to better steady-state performance and a constant switching frequency. Despite its many benefits, there are some limitations associated with the MPC-DSVM algorithm. One of the primary limitations is its high computational burden, which can be challenging to

manage, particularly in low-speed microprocessors [8]. In addition, initializing the lookup tables for a large number of virtual voltage vectors requires additional computation time. In [9], a new approach called single-layer neural network-based model predictive control with discrete space vector PWM (SLNN-MPC-DSVPWM). This approach uses a simple neural network that is trained using an advanced algorithm called the Levenberg-Marquardt algorithm to overcome the limitations of MPC-DSVM. The proposed SLNN-MPC-DSVPWM method offers several advantages over previous methods. It is relatively easy to implement on low-order digital signal processors (DSPs), allowing the use of a large number of virtual voltage vectors with low computation time and without the need for lookup table initialization However, it has not been evaluated for parameter variations, which may affect its overall performance.

Recently, Model-Free Predictive Current Control Method (MFPCC) has been gaining attention as a more efficient solution for controlling systems. The advantage of this method is that it does not require prior knowledge of the system model, making it less susceptible to variations in parameters. This makes MFPCC a more efficient and practical solution. The MFPCC method was introduced for PMSM drives and uses two lookup tables (LUTs) to store data on the changes in dq currents caused by applying different voltage vectors [10]. The optimal voltage vector is then selected based on a pre-defined cost function. However, if the same voltage vector is not applied repeatedly, the stored information becomes outdated and can result in current stagnation, affecting the performance of the control. In [11], another MFPCC approach based on an ultra-local model has been proposed for PMSM drives. The improved version of this method is employed then with an extended state observer [12], and applied later for DFIG drives [13], [14]. However, most of MFPCC schemes suffer either from the stagnation problem or the poor control performance [15].

Due to the above advantages and limitations of each method, a fast dynamic FOC (FFOC) for PMSM based on a direct real VVs and hysteresis switch is proposed. The proposed method uses the rotor position of the motor to select a direct real VVs without the need for high computation time for cost function and prediction model of MPC. Then, using hysteresis switch, when the error is larger than the high band of the hysteresis switch, this activates the use of direct real VVs based on the rotor position to quickly reach $I_q$ to the neighborhood of their reference values. When the error is lower than the low band of the hysteresis switch, the system is near to reference point. Consequently, the hysteresis method switches from real VVs to FOC. Simulation results proved that the FFOC has similar steady-state performance as FOC. In addition, FFOC shows faster dynamic performance than FOC and FOC-MPC hybrid method [16][17].

## II. Field-Oriented Control

In this study, a surface Mount PMSM is used, which is fed by a two-level voltage source inverter as shown in Fig 1. The mathematical equations that describe the voltage behavior of the PMSM in the d-q reference frame of the rotor, utilizing FOC techniques, are described in equation (1) [18].

$$\begin{cases} v_{dr} = k_{pd} I_{dErr} + k_i I_{dIErr} T_{samp} - \omega_{ee} L_q I_{qr} \\ v_{qr} = k_{pq} I_{qErr} + k_i I_{qIErr} T_{samp} + \omega_{ee} L_d I_{dr} + \omega_e \ \phi_f \end{cases}, \quad (1)$$

where $V_{dr}$, and $V_{qr}$ are the voltage components of the *d-q* rotating frame. $I_{dErr}$, $I_{qErr}$, $I_{dIErr}$, $I_{qIErr}$, $I_{dr}$, and $I_{qr}$ are the error, integration error, and estimated current components in the *d-q* rotating frame, respectively. $L_d$ and $L_q$ are the inductances, $\omega_e$ is the electrical rotor speed, and $\varphi_f$ is the flux linkage established by the rotor. $k_{pg}$ and $k_{ig}$ are the proportional and integral gains, respectively, which are calculated as in (2),

$$\begin{cases} k_{pdg} = L_d \omega_{bcc} \\ k_{pqg} = L_q \omega_{bcc} \\ k_{ig} = R_{ss} \omega_{bcc} \end{cases}, \quad (2)$$

where $\omega_{bcc}$ is the bandwidth for current control and $R_{ss}$ is the stator resistance of the motor.

$V_{dr}$, and $V_{qr}$ describe the voltage behavior of the PMSM in the rotor reference frame transformed into stationary reference as described in equation (3). This transformation allows for the analysis of the PMSM in the stationary reference frame, which can simplify the analysis of the motor and its control system.

$$\begin{cases} v_\alpha = v_{dr} \cos(\theta_{rr}) - v_{qr} \sin(\theta_{rr}) \\ v_\beta = v_{dr} \cos(\theta_{rr}) + v_{qr} \sin(\theta_{rr}) \end{cases}, \quad (3)$$

In order to estimate the rotor position of the PMSM, an encoder can be attached to the motor. This estimated position, denoted by $\theta_{rr}$, is utilized in the generation of switching signals for the two-level inverter using SVPWM. Specifically, the ABC components of equation (3) are compared with the PWM carrier, and the resulting comparison generates the necessary switching signals for the two-level inverter.

## III. Proposed Fast Dynamic FOC

The fast dynamic FOC (FFOC) uses the rotor position of the motor to select a direct large VVs without the need for high computation time for cost function and prediction model of MPC as shown in Fig.2 and Table 1. For example, when rotor position is equal 0 to 1.047, $V_3$ is implemented. Direct VVs based on rotor position has less complexity and faster dynamic response compared with MPC. In addition, direct real VVs does not affect by parameter variation of the model. Hysteresis switch is implemented to switch between FOC and direct real VVs. A hysteresis controller used in this study is described by two bands, which are denoted by $J_h$ and $J_l$. $J_h$ is high band while $J_l$ is low band. The hysteresis controller can have one

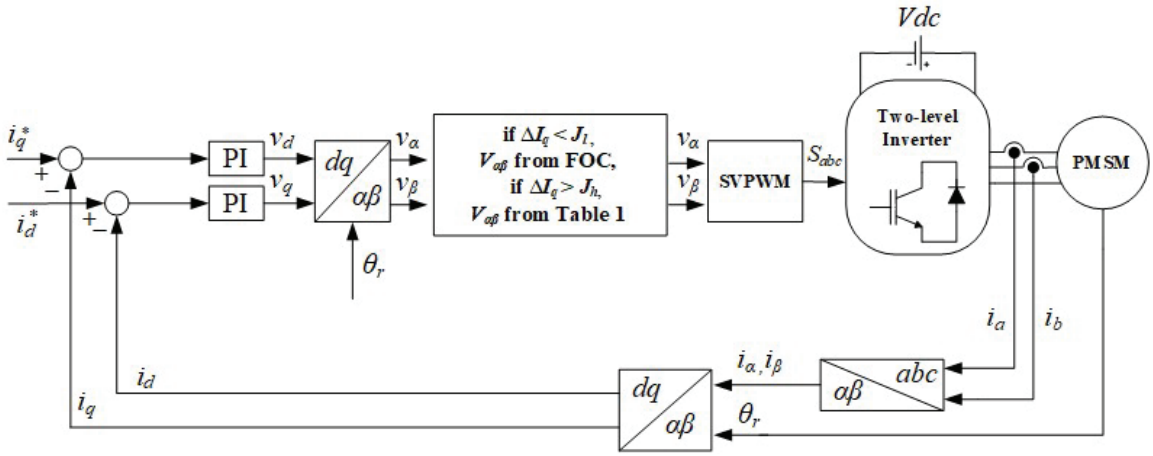


Fig. 2. Block diagram of the proposed FFOC.

of two output states, which are determined by the input signals and the position of the reference trajectory relative to the two bands. The selection of the appropriate hysteresis controller is determined by a set of rules, as described in equation (4).

$$\begin{cases} \text{FOC}, & if \quad \Delta I_q \le J_l \\ \text{Direct real VV}_S, & \Delta I_q \ge J_h \end{cases} \tag{4}$$

When $\Delta I_q \ge J_h$, the control system switches to direct real $VV_S$ in order to rapidly move the system states to the vicinity of their reference values. On the other hand, when $\Delta I_q \le J_l$, the system is considered to be close to its operational point, and the control system switches from direct real $VV_S$ to FOC. In order to simplify switching methods, the control system apply the same switch in the previous time step k-1. This ensures a smooth and efficient control system operation while avoiding unnecessary commutations between control schemes. The block diagram of the proposed FFOC is shown in Fig 2.

## IV. Simulation Results

The simulation results were done using PSIM software and parameter of PMSM is shown in Table 2. For fair performance comparison, FOC, FOC-MPC, and proposed FFOC were evaluated during nominal parameter at 300 r/min and $I_q$ step change from 1 to 5A. The sampling time was $T_{sam}$ = 100 µs. As shown in Fig 3, these three methods exhibit good steady-state performance. However, FOC shows a longer rise time of 3.5 ms as compared to the FOC-MPC and FFOC. FFOC has a faster dynamic response with 1.1 ms compared to the FOC-MPC with 1.2 ms due to the direct real VVs are implemented without the need for high computation time of MPC. Fig 4 shows the simulation result of the performance of MPC with nominal parameters and under the influence of parameter variation ($0.5xL_d$ and $0.5xL_q$). The reference speed is set to 900r/min $I_q$ step change from 1 to 10A. MPC shows a fast dynamic response with 1ms under the ideal parameter as shown in Fig 4a. However, steady-state and transient state are affected under parameter variation as shown in Fig 4b. MPC has a slow dynamic response with 1.3ms compared with 1ms for MPC at nominal parameters. In addition, it is clear that $I_q$ ripples is also increased compared with MPC at nominal parameters.

FOC, FOC-MPC, and the proposed FFOC are evaluated at the same conditions of MPC at nominal parameters and parameter variation in order to evaluate their dynamic performance as shown in Figs 5 and 6. From the simulation results, it is clearly shown that MPC has faster dynamic performance with 1 and 1.3 ms compared with FOC with 3.6 and 5.6 at nominal parameter and parameter variation respectively, In contrast, FOC has better steady-state performance compared with MPC at nominal parameter and parameter variation. FOC-MPC and proposed FFOC show better steady-state performance compared with MPC and FOC by combining good steady-state and fast dynamic performance. However, the proposed FFOC shows better robustness under parameter variation compared with FOC-MPC as shown in Fig 6.

TABLE I
VOLTAGE VECTORS SELECTION USING ROTOR POSITION

| Voltage Vector ($V_Z$) | $V_z=V_\alpha+jV_\beta$ | Rotor Position ( $\theta_r$ ) |
|---|---|---|
| $V_1$ | $\frac{2}{3}V_{dc}$ | $4.188 <= \theta_r < 5.235$ |
| $V_2$ | $\frac{1}{3}V_{dc}+j\frac{\sqrt{3}}{3}V_{dc}$ | $5.235 <= \theta_r < 6.283$ |
| $V_3$ | $-\frac{1}{3}V_{dc}+j\frac{\sqrt{3}}{3}V_{dc}$ | $0.00 <= \theta_r < 1.047$ |
| $V_4$ | $-\frac{2}{3}V_{dc}$ | $1.047 <= \theta_r < 2.094$ |
| $V_5$ | $-\frac{1}{3}V_{dc}-j\frac{\sqrt{3}}{3}V_{dc}$ | $2.094 <= \theta_r < 3.141$ |
| $V_6$ | $\frac{1}{3}V_{dc}-j\frac{\sqrt{3}}{3}V_{dc}$ | $3.141 <= \theta_r < 4.188$ |

FFOC shows faster dynamic performance with 0.8ms compared with 1.3ms for FOC-MPC at the influence of parameter variations. In addition, during the nominal

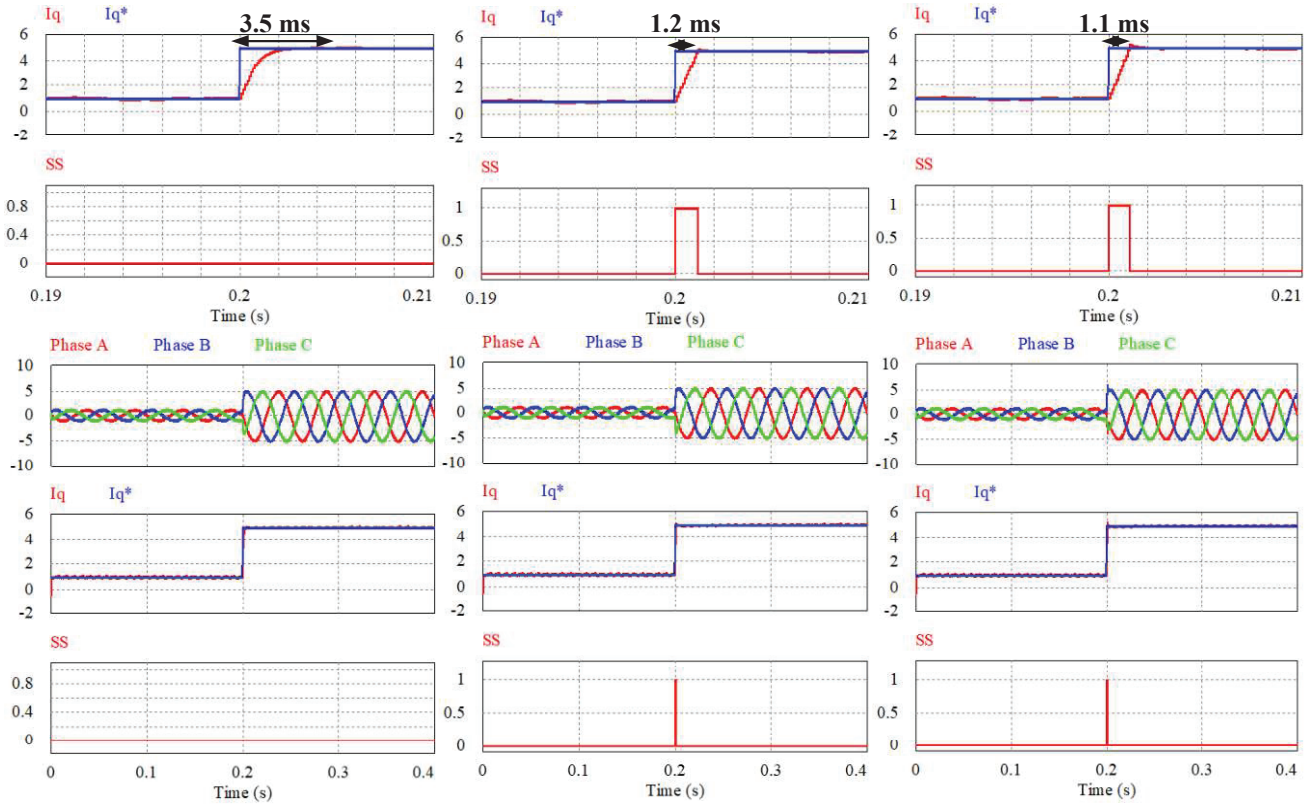


Fig. **3**: Simulation results of different control methods during nominal parameter at 300 r/min ($I_q$* = 1 to 5A) (a) FOC. (b) FOC-MPC. (c) FFOC.

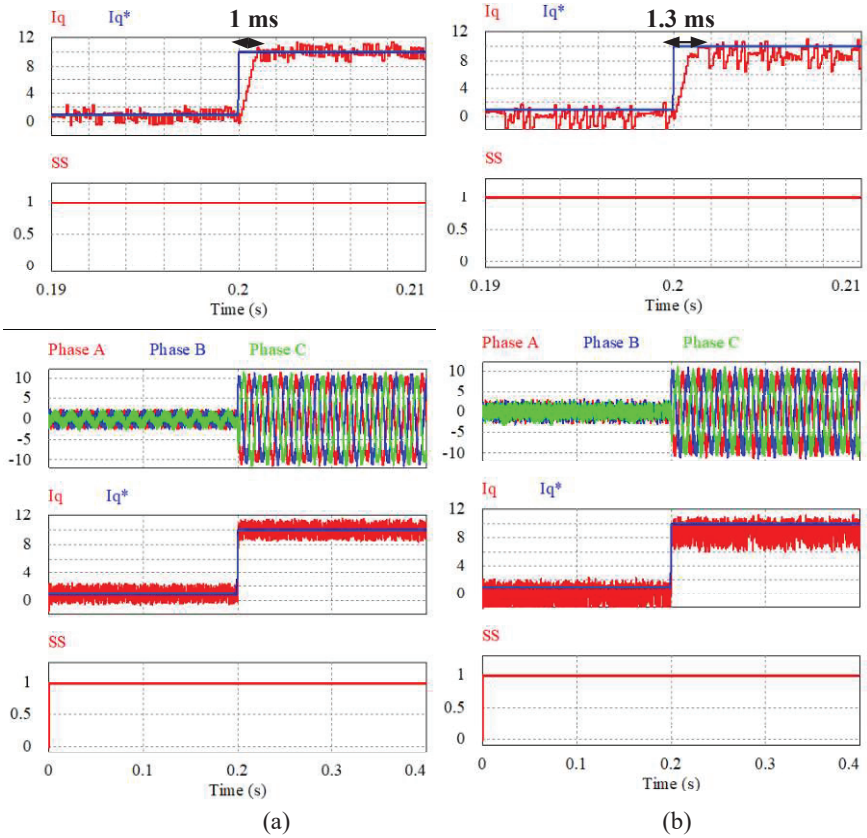


Fig. 4: Simulation results of MPC control method at 900 r/min ($I_q$* = 1 to 10A) (a) At nominal parameter. (b) At Parameter variation (0.5x$L_d$ and 0.5x$L_q$).

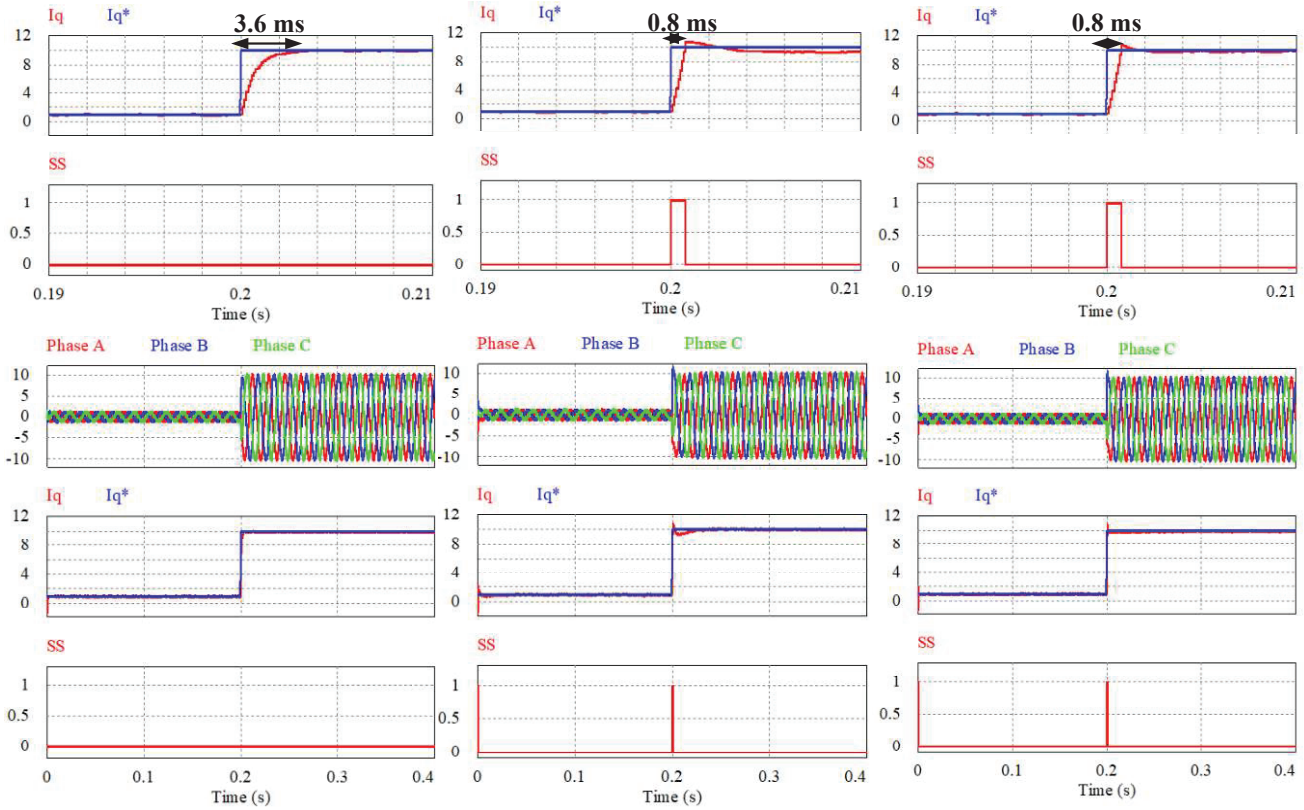


Fig. 5: Simulation results of different control methods during nominal parameter at 900 r/min ($I_q$* = 1 to 10A) (a) FOC. (b) FOC-MPC. (c) FFOC.

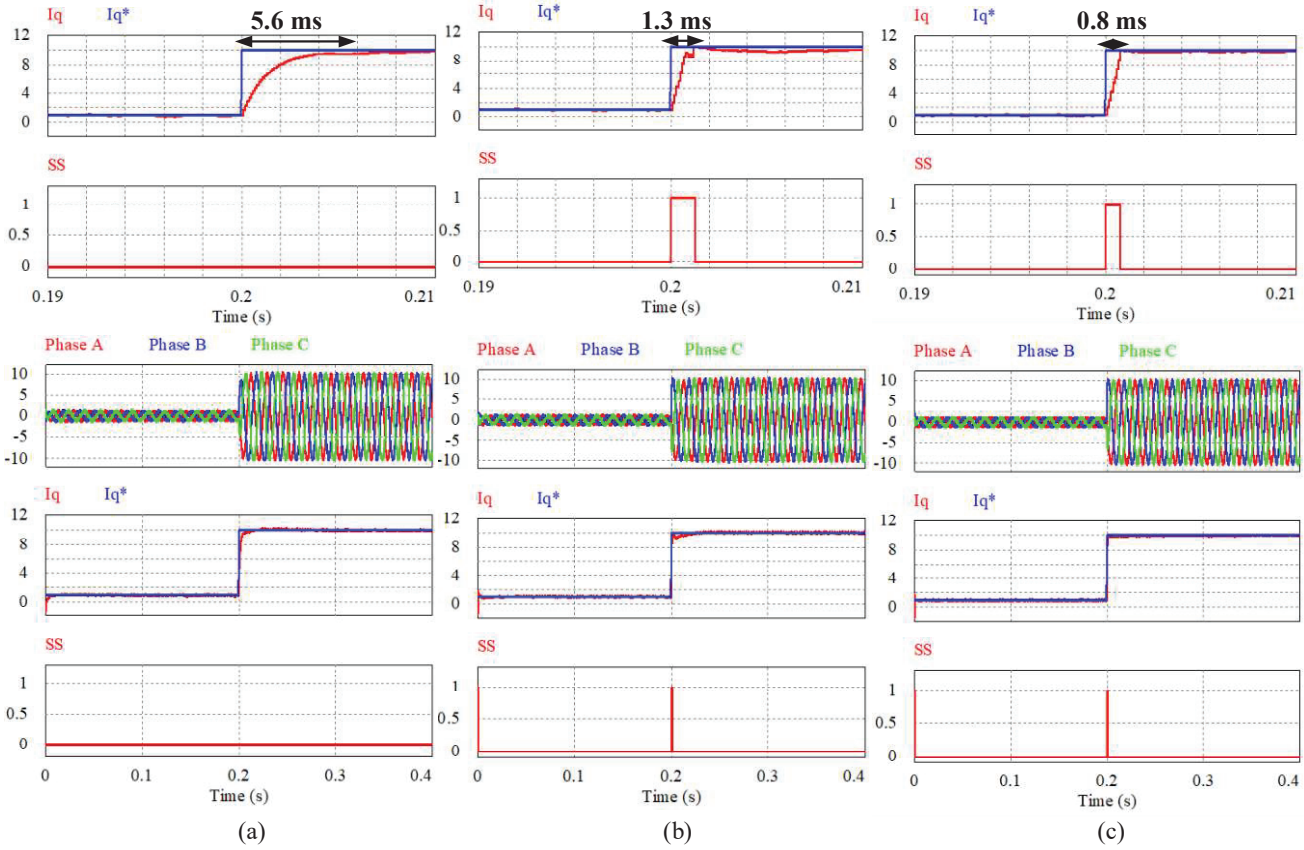


Fig. 6: Simulation results of different control methods during parameter variation at 900 r/min ($I_q$* = 1 to 10A) (a) FOC. (b) FOC-MPC. (c) FFOC.

parameter, both FOC-MPC and FFOC show the same dynamic performance with 0.8ms as shown in Fig 5.

## V. Conclusions

In this article, a fast dynamic FOC is proposed to solve the limitation of conventional FOC which has slow dynamic response. FFOC uses the FOC in steady-state and the direct real VVs in transient-state. The direct real VVs is generated based on the rotor position of the motor without the need for high computation time of MPC. Then, the hysteresis switch is used to switch between controllers. Simulations results proved that the proposed FFOC improved the dynamic performance of FOC and outperformed FOC-MPC in terms of complexity. In addition, FFOC has better robustness under parameter variations compared with FFOC-MPC and MPC which are highly affected by parameter variation during steady-state and dynamic performance. One drawback of the proposed FFOC could be faced during experiment implementation is the large overshoot which could be solved by calculated the $I_q$ average ripples and select optimal percentage error that prevent to select the direct VVs when the $I_q$ is near to the reference or by applying fuzzy logic to select direct VVs instead of hysterias method .

TABLE II
Simulation Parameters

| Parameters | Value |
|---|---|
| DC-link voltage ($V_{dc}$) | 600V |
| Rated Power | 5kw |
| Pole ($P$) | 8 |
| Inertia ($J$) | 0.00666Kg·m$^2$ |
| d-axis inductance ($L_d$) | 0.00729H |
| q-axis inductance ($L_q$) | 0.00725H |
| Stator resistance ($R_s$) | 0.158Ω |
| Magnetic flux linkage ($\varphi_f$) | 0.264Wb |
| Rated speed | 1750rpm |
| Sampling time ($T_{samp}$) | 100μs |

## Acknowledgment

This work was supported by the Korea Institute of Energy Technology Evaluation and Planning (KETEP) and the Ministry of Trade, Industry & Energy (MOTIE) of the Republic of Korea (No. 20206910100160).

## References

[1] S. S. Hakami and K.-B. Lee, "Four-level hysteresis-based DTC for torque capability improvement of IPMSM fed by three-level NPC inverter," *Electronics*, vol. 9, no. 10, p. 1558, 2020.

[2] Sadeq Ali Qasem Mohammed, and K.-B. Lee, "Improved adaptive iterative learning current control approach for IPMSM drives," *J. Power Electron*., vol. 23, pp. 284–295, 2023.

[3] Y. Zhang and J. Zhu, "Direct torque control of permanent magnet synchronous motor with reduced torque ripple and commutation frequency," *IEEE Trans. Power Electron*., vol. 26, no. 1, pp. 235–248, Jan. 2011.

[4] Y. Zhang, D. Xu, J. Liu, S. Gao, and W. Xu, "Performance improvement of model-predictive current control of permanent magnet synchronous motor drives," *IEEE Trans. Ind. Appl*., vol. 53, no. 4, pp. 3683–3695,Jul./Aug. 2017.

[5] D. Casadei, F. Profumo, G. Serra, and A. Tani, "FOC and DTC: two viable schemes for induction motors torque control*," IEEE Trans. Power Electron*., vol. 17, no. 5, pp. 779–787, Sep. 2002.

[6] Y. Inoue, S. Morimoto, and M. Sanada, "Comparative study of PMSM drive systems based on current control and direct torque control in flux weakening control region," *IEEE Trans*. Ind. Appl., vol. 48, no. 6, pp.2382–2389, Nov. 2012.

[7] J. Rodriguez et al., "Latest advances of model predictive control in electrical drives—part I: basic concepts and advanced strategies," *IEEE Trans. Power Electron*., vol. 37, no. 4, pp. 3927-3942, April 2022.

[8] H. Moon, J. Lee, and K.-B. Lee, "A robust deadbeat finite set model predictive current control based on discrete space vector modulation for a grid-connected voltage source inverter," *IEEE Trans. Energy Convers*., vol. 33, no. 4, pp. 1719–1728, Dec. 2018.

[9] H. A. G. Al-Kaf and K.-B. Lee, "Low Complexity MPC-DSVPWM for Current Control of PMSM Using Neural Network Approach," *IEEE Access*, vol. 10, pp. 132596-132607, 2022.

[10] C. Lin, T. Liu, J. Yu, L. Fu, and C. Hsiao, "Model-free predictive current control for interior permanent-magnet synchronous motor drives based on current difference detection technique", *IEEE Trans. Ind. Electron*., vol. 61, no. 2, pp. 667–681, Feb. 2014.

[11] Y. Zhou, H. Li, and H. Yao, "Model-free control of surface mounted PMSM drive system", *in 2016 IEEE International Conference on Industrial Technology (*ICIT), March 2016, pp. 175–180.

[12] Y. Zhang, J. Jin and L. Huang, "Model-free predictive current control of PMSM drives based on extended state observer using ultra local model", *IEEE Trans. Ind. Electron*., vol. 68, no. 2, pp. 993-1003, Feb. 2021.

[13] Y. Zhang, T. Jiang and J. Jiao, "Model-free predictive current control of a DFIG Using an ultra-local model for grid synchronization and power regulation", *IEEE Trans. Energy Conv*., vol. 35, no. 4, pp. 2269-2280, Dec. 2020.

[14] Y. Zhang, T. Jiang and J. Jiao, "Model-free predictive current control of DFIG based on an extended state observer under unbalanced and distorted grid", *IEEE Trans. Power Electron.*, vol. 35, no. 8, pp. 8130- 8139, Aug. 2020.

[15] H. Mesai Ahmed, I. Jlassi, A. J. Marques Cardoso and A. Bentaallah, "Model-Free Predictive Current Control of Synchronous Reluctance Motors Based on a Recurrent Neural Network," IEEE *Trans. Ind. Electron*., vol. 69, no. 11, pp. 10984-10992, Nov. 2022.

[16] H. A. G. Al-Kaf, and K.-B. Lee,"Robust Hybrid Current Controller for Permanent-Magnet Synchronous Motors," J. Electr. Eng. Technol., Jan. 2023.

[17] H. A. G. Al-kaf, S. S. Hakami and K. -B. Lee, "Hybrid current controller for permanent-magnet synchronous motors using robust switching techniques," *IEEE Trans. Power Electron*., vol. 38, no. 3, pp. 3711-3724, Mar. 2023.

[18] L. M. Halabi, I. M. Alsofyani, and K. B. Lee, "Multiple-fault-tolerant strategy for three-phase hybrid active neutral point clamped converters using enhanced space vector modulation technique," *IEEE Access*, vol. 8, pp. 180113–180123, 2020.